Heliyon 9 (2023) e21092

Contents lists available at ScienceDirect

Heliyon

journal homepage: www.cell.com/heliyon

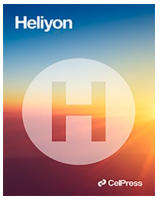

Identification and validation of molecular subtypes' characteristics in bladder urothelial carcinoma based on autophagy-dependent ferroptosis

Shiwei Liu [a,b,e,f,1], Jing Zhai [c,1], Deng Li [b,1], Yu Peng [c], Yi Wang [b,d,**], Bo Dai [a,e,f,*]

[a] Department of Urology, Fudan University Shanghai Cancer Center, Shanghai, 200032, China
[b] Department of Urology, Shanghai General Hospital, Shanghai Jiao Tong University School of Medicine, Shanghai, 200080, China
[c] Department of Urology, Yueyang Hospital of Integrated Traditional Chinese and Western Medicine, Shanghai University of Traditional Chinese Medicine, Shanghai, 200437, China
[d] Department of Urology, Affiliated Hospital of Nantong University, Nantong, 226001, Jiangsu Province, China
[e] Department of Oncology, Shanghai Medical College, Fudan University, Shanghai, 200032, China
[f] Shanghai Genitourinary Cancer Institute, Shanghai, 200032, China

ARTICLE INFO

Keywords:
Autophagy-dependent ferroptosis
Bladder urothelial carcinoma
Immunotherapy
Prognosis

ABSTRACT

Background: Nowadays, more evidences indicated that autophagy-dependent ferroptosis regulatory molecules (ADFRMs) may be closely related to various tumors. In current study, we intended to establish a prognostic ADFRMs signature and investigated its potential roles in bladder urothelial carcinoma (BLCA).

Methods: Two distinct clusters were determined by consensus clustering with expression of 119 identified ADFRMs in BLCA. The tumor microenvironment was investigated through "CIBERSORT" algorithm, and enrichment analyses were utilized to seek molecular characteristics of differentially expressed genes (DEGs) between clusters. Moreover, a 2-ADFRMs prognostic signature including TRIB3 and WIPI1 was identified in TCGA cohort and further evaluated in the GSE13507 cohort. The qRT-PCR was conducted to examine the expression of prognostic genes. Further, the risk score was gained through calculating the level of TRIB3 and WIPI1 expression through the coefficient. The correlations between risk score with clinicopathologica features, tumor microenvironment, and drug sensitivity were explored.

Results: Patients in TCGA-BLCA were grouped into two clusters with different expression patterns of ADFRMs. And the overall survival, tumor microenvironment and biological functions were significant different between two clusters. Moreover, a 2-ADFRMs model was constructed, and patients were separated into a low-risk and high-risk group. Survival analysis indicated patients with low risk promised a good prognosis, suggesting the risk score determined with ADFRMs signature exhibited an acceptable capacity for survival prediction in BLCA. Correlation analysis

Abbreviations: ADFRM, Autophagy-dependent ferroptosis regulatory molecules; BLCA, Bladder urothelial carcinoma; TCGA, The Cancer Genome Atlas; GSEA, Gene set enrichment analysis; OS, Overall survival; NES, Normalized enrichment score; IC50, half maximal inhibitory concentration; ROC, receiver operating characteristic curve; DEGs, differentially expressed genes; CDF, cumulative distribution function.

* Corresponding author. Department of Urology, Fudan University Shanghai Cancer Center, No. 270 Dongan Road, Xuhui District, Shanghai, 200032, China.

** Corresponding author. Department of Urology, Shanghai General Hospital, Shanghai Jiao Tong University School of Medicine, No.85 Wujin Road, Hongkou District, Shanghai, 200080, China.

E-mail addresses: wangyi_urology@163.com (Y. Wang), bodai1978@126.com (B. Dai).

[1] **Shiwei Liu**, **Jing Zhai**, **Deng Li** contributed equally to this work.

https://doi.org/10.1016/j.heliyon.2023.e21092
Received 2 February 2023; Received in revised form 11 September 2023; Accepted 16 October 2023
Available online 18 October 2023

demonstrated risk score had close ties with age, stage, and tumor microenvironment. In vivo, the expression of prognostic genes was identified to be up-regulated in BLCA cell line T24.
Conclusion: The constructed 2-ADFRMs signature was a promising model to predict prognosis and correlated with tumor microenvironment, which had latent clinical value in the intervention for BLCA.

1. Introduction

Bladder urothelial carcinoma (BLCA), was one of the most common malignant neoplasms in urinary system, and 91,893 vs 81,180 estimated new BLCA cases and 42,973 vs 17,100 BLCA relevant deaths were reported in China and United States in 2022, respectively [1,2]. As a complicated disease, BLCA has a high mortality and morbidity rates if not treated promptly and optimally [3]. Despite encouraging progress being achieved in the treatment of BLCA, the overall survival (OS) of BLCA patients especially for those with advanced stage remains to be unsatisfactory [4,5]. Therefore, identifying for new effective indicators and therapeutic strategies to enhance the prognosis for BLCA is critical.

Ferroptosis, deemed as a newly defined type of cell death, was distinguish from necrosis, apoptosis, and autophagy at the genetic, biochemical, and morphological levels [6]. An increasing number of reports regarding ferroptosis have been immensely extended and the thorough understanding of ferroptosis has been constantly progressing, which was closely related to the etiopathology of several diseases including cancer disease [7]. As reported, ferroptosis was discovered as a nonnegligible role in suppression and immunity of tumor, implying a huge potential for cancer treatment [8]. In recent years, increasing evidence claimed that the autophagic-related mechanism, to a large extent, contributed to ferroptosis [9,10]. The pathway, which may contribute to tissue fibrosis, inflammation responses, and anticancer therapies, was referred to as autophagy-dependent ferroptosis [11]. The mechanism of autophagy-dependent ferroptosis offered a new insight for the study of ferroptosis in tumors, and a profound understanding of it may be more meaningful for anti-cancer therapy. However, the current studies of autophagy-dependent ferroptosis on tumors, including BLCA, were still limited, and we urged to investigate its relationship with tumor progression and prognosis in BLCA.

In this paper, a prognostic model involving autophagy-dependent ferroptosis regulatory molecules (ADFRMs) was constructed for BLCA. We assessed the expression level of ADFRMs in TCGA-BLCA, and patients were grouped into two clusters with its expression level. Further, one risk prognostic model was developed with the ADFRMs. To assess its prognostic and immunotherapeutic value in BLCA patients, the molecular and immune characteristic of the signature were also explored. These findings provided new perspectives for the diagnosis, prognosis and immunotherapy for BLCA from the view of autophagy-dependent ferroptosis.

2. Materials and methods

2.1. Raw data acquiring and processing

The RNA sequencing (RNA-seq) profiles, gene mutation data, as well as clinical information from 409 bladder cancers and 19 normal adjacent tissues were retrieved in TCGA database (http://cancergenome.nih.gov/). The GSE13507 data set including the total RNA-seq and the clinical data for BLCA samples were obtained from GEO database (https://www.ncbi.nlm.nih.gov/geo/), which was regarded as the external cohort for further validation. The samples with missing clinical data were removed in further analysis. These data were normalized and processed in a R statistical environment for further analysis, as previously described [12].

2.2. Consensus cluster analysis for 119 ADFRMs

The “ADFRMs” set was identified from two online databases, including the “HAMdb” (hamdb.scbdd.com/home/index/) and the “FerrDb” (www.zhounan.org/ferrdb/current/). Ultimately, total 119 ADFRMs were included in current study. Based on the expression level of 119 ADFRMs, the consensus classification was carried out to identify the distinct ADFRMs patterns in TCGA-BLCA, and patients were grouped into two clusters through R “ConsensusClusterPlus”. The curve of CDF (Cumulative Distribution Function) was utilized to determine an optimal number of clustering [13], and ultimately $k = 2$ was claimed to own the best stability of the clustering, based on which subsequent analysis were performed. The OS curve analysis was conducted to identify their survival characteristics using the “Survminer” R package.

2.3. Differential gene expression and functional analysis

To determine the differentially expressed genes (DEGs), the RNA-seq data of TCGA-BLCA were analyzed through the “limma” R package, with the following selection criteria of $|\log_2 FC \text{ (fold change)}| > 1$ and FDR (false discovery rate) < 0.05, and the outcome was visualized with “pheatmap” R package. The GO (Gene Ontology) as well as KEGG (Kyoto Encyclopedia of Genes and Genomes) analysis were carried out to investigate the enrichment of DEGs using the “clusterProfiler”, “enrichplot” and “GOplot” package of R respectively. GSEA (Gene Set Enrichment Analysis) was further applied to explore the potential biological functions of different subgroups constructed by the consensus classification in TCGA-BLCA [14]. The p value less than 0.05 were thought to be significant.

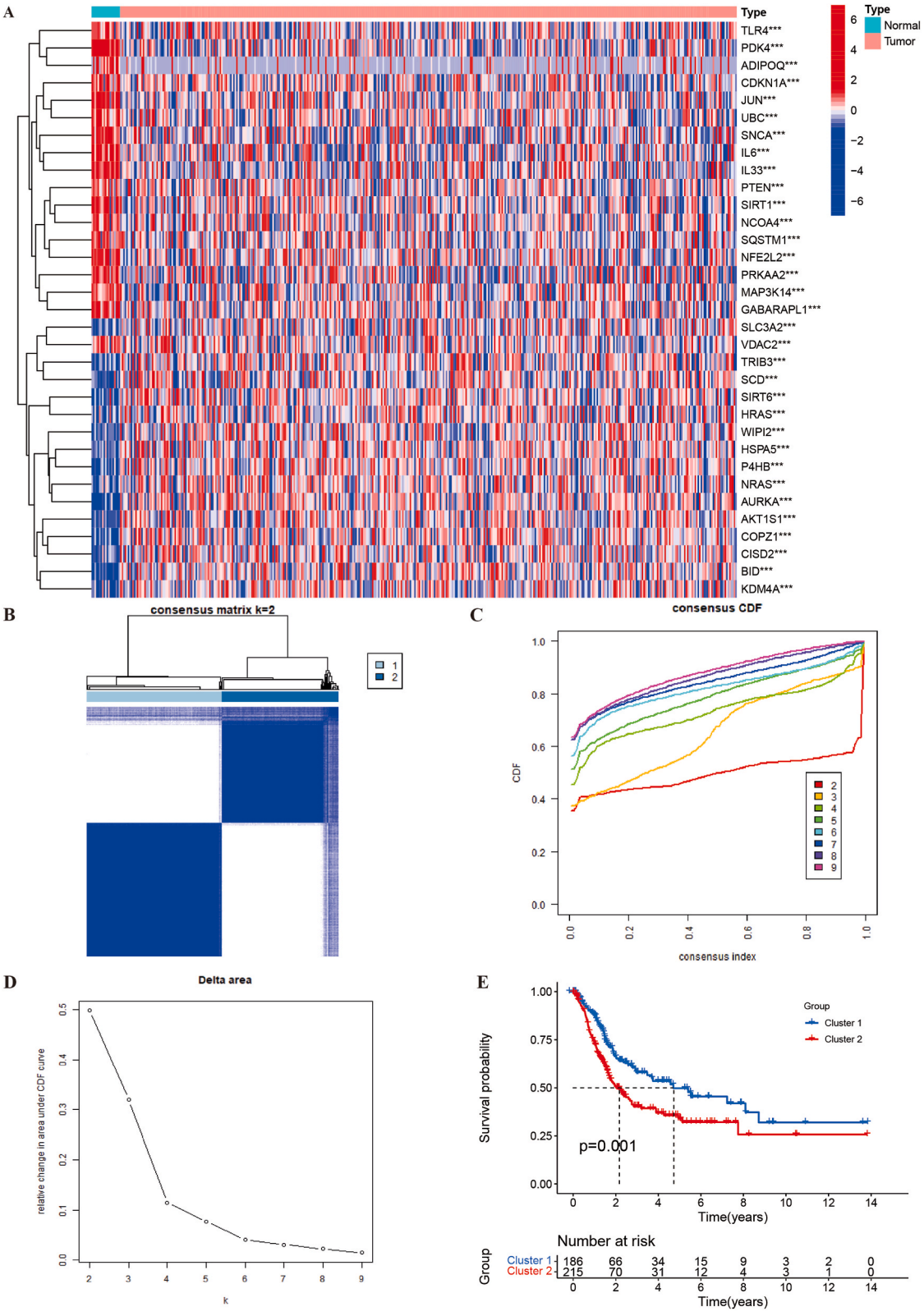

Fig. 1. Expression pattern of ADFRMs and consensus clustering analysis in BLCA. (A) The expression level of 33 differentially expressed ADFRMs between BLCA and adjacent normal tissues with heatmap. (B) Consensus clusters of BLCA patients with k = 2. (C) CDF of consensus clusters with k = 2 to 9. (D) The curve of consensus clustering CDF. (E) The OS prognostic analysis between two clusters. ***p < 0.001.

2.4. Establishment and validation of a prognostic model

Through the Univariate Cox regression algorithm, three genes of 119 ADFRMs were identified as independent factors to predict prognosis which were further utilized to establish the ADFRMs signature in BLCA. Further, the lasso (Least absolute shrinkage and selection operator) logistics tool was conducted to determine the most outstanding markers to construct a prognostic model. Ultimately, a two-ADFRMs prognostic model including TRIB3 and WIPI1 for BLCA was constructed. The risk score was gained through calculating the expression level of TRIB3 and WIPI1 through the coefficient. Then, the samples in TCGA-BLCA and GSE13507 cohort were separated into a low-risk and high-risk group with the median cut-off value respectively. The OS curve analysis were then conducted using R "Survminer" to determine the survival characteristic, and the time-dependent ROC analysis was carried out to assess its prediction accuracy through R package "survival" and "timeROC". Univariable and multivariable Cox analysis were conducted to evaluate if the identified ADFRMs signature could be an independent prognostic parameter as well as the clinical information including age, gender, grade and stage. Besides, the correlation analyses between the risk score and clinicopathological information were further conducted, and the Wilcoxon rank sum and Kruskal-Wallis test were utilized for the comparison.

2.5. Analysis of immune and molecular characteristics between two clusters

The tumor microenvironment, containing the immune and stromal scores of BLCA patients was formulated using TCGA-BLCA RNA-seq data by means of the "ESTIMATE" algorithm [15]. The TIMER website was utilized to investigate the immune cell infiltration levels between two clusters in BLCA. The database "cBioPortal" was utilized to acquire the genetic alteration information as well as the quantity and quality of genetic mutations between two groups. Besides, the algorithm "CIBERSORT" was performed to quantify relative concentration of 22 immune cell types fraction, and their scores were compared between the two clusters further. And the immune cells proportions and clinical characteristic were compared between two subgroups, the results were illustrated with the landscape map. Besides, the algorithm "ssGSEA" was performed to quantify relative concentration of 28 immune cell types fraction, and their scores were compared between the two subgroups.

2.6. Drug sensitivity of prognostic genes

We obtained the mRNA expression level of NCI-60 human tumor cell lines from "CellMiner" dataset (https://discover.nci.nih.gov/cellminer/). The correlation of prognostic genes and drug sensitivity was investigated by the Pearson correlation analysis.

2.7. RNA extraction and real-time qPCR

Total RNAs of BLCA cell line T24 and normal bladder cell line SV-HUC-1 were acquired by TRIzol. PrimeScript RT reagent kit (Novabio, China) was utilized to synthesize the complementary DNA. RT-qPCR was conducted to identify relative expression of target genes via SYBR green, and was further analyzed through StepOne Software v2.3. The relative levels were normalized through expression of ACTB. The primer sequences were list as follow: ACTB primer:5′-CATGTACGTTGCTATCCAGGC-3' (forward); 5′-CTCCTTAATGTCACGCACGAT-3.

'(reverse); TRIB3 primer:5′-GCTTTGTCTTCGCTGACCGTGA-3' (forward); 5′-CTGAGTATCT.

CAGGTCCCACGT-3' (reverse); WIPI1 primer: 5′-CTTCAAGCTGGAACAGGTCACC-3' (forward); 5′-CGGA-GAAGTTCAAGCGTGCAGT' (reverse).

2.8. Statistical analysis

All statistical analysis were carried out through "R" v 4.2.1. The "Wilcoxon" test was applied for comparing the differences of two subgroups. The p value less than 0.05 was deemed as statistically significant.

3. Results

3.1. Expression pattern of ADFRMs and consensus clustering analysis in BLCA

To investigate potential influence of ADFRMs on BLCA, the expression level of 119 identified ADFRMs were systematically analyzed between BLCA and adjacent normal tissues. The results were presented in Fig. 1A, total 33 ADFRMs, inclusive of 15 up-regulated ADFRMs and 18 down-regulated ADFRMs, were determined as differentially expressed ADFRMs in BLCA (**$p < 0.05$**). Then, one consensus classification was carried out to identify the vintage number of clusters in TCGA-BLCA. Eventually, $k = 2$ was considered to have the optimal clustering stability (Fig. 1B–D), and patients in BLCA cohort were grouped into two clusters based on the ADFRMs expression pattern. Further, one prognostic analysis was conducted between two clusters, which indicated the OS of BLCA patients in cluster 1 was markedly longer than those in cluster 2 (Fig. 1E, $p = 0.001$).

3.2. Tumor microenvironment analysis of clusters based on ADFRMs in BLCA

Increasing evidences demonstrated the strict relationship between tumor microenvironment and the malignant degree. To further

investigate the correlations between the ADFRMs and tumor microenvironment in BLCA, the level of immune cell infiltration in TCGA-BLCA was identified through "CIBERSORT" algorithm. Fig. 2A indicated there were significant differences in the proportions of immune cells between two subgroups, including plasma cells, B cells naive, T cells regulatory, T cells gamma delta and etc (**p < 0.05**). Next, we identified the expression level immune checkpoint blockade genes between two clusters. As displayed in Fig. 2B and eight immune checkpoint blockade genes were identified significantly differential between two clusters. Interestingly, all of immune

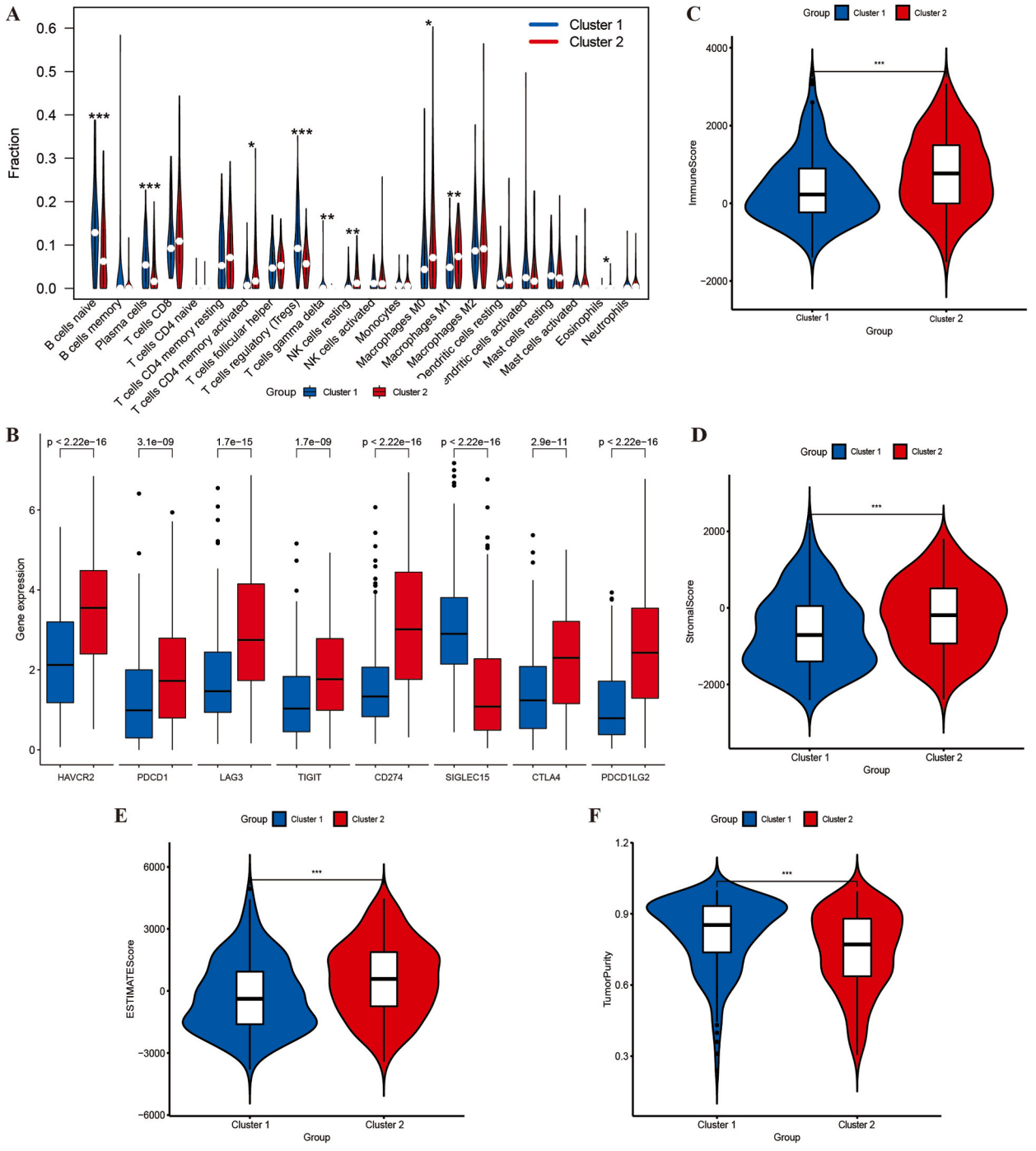

Fig. 2. Tumor microenvironment analysis of clusters based on ADFRMs in BLCA. (A) Immune cell infiltrates level of BLCA patients between two clusters with violin plot. (B) Immune checkpoints blockage genes expression level of BLCA patiens between two clusters with boxplots. (*C*–F) The analysis of ESTIMATE score, Immune score, Stroma score and Tumor purity between two clusters in BLCA. *p < 0.05, **p < 0.01, and ***p < 0.001.

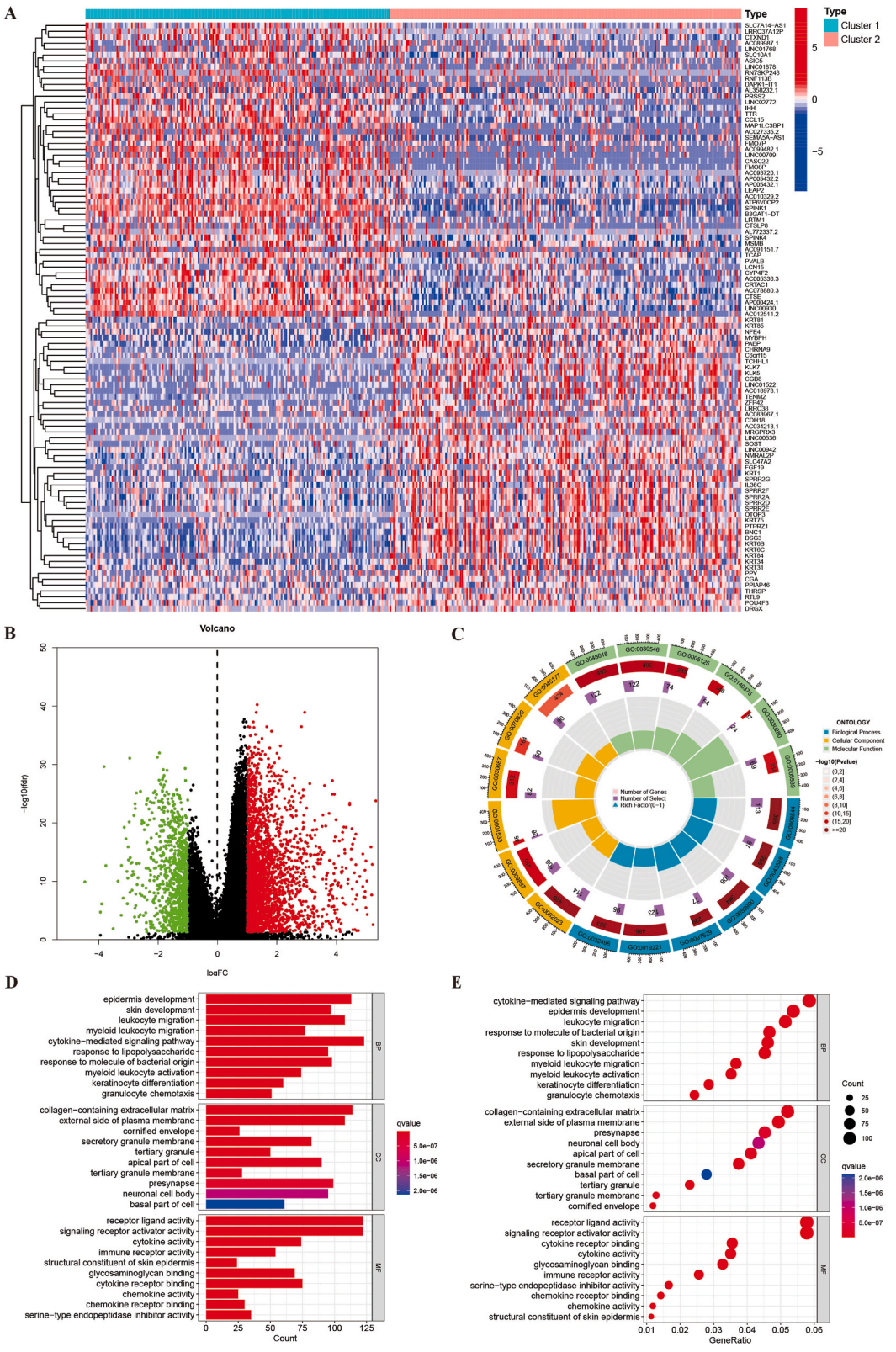

Fig. 3. Correlation analysis between ADFRMs with molecular characteristics. (A–B) The identified DEGs between two clusters with heatmap and volcano plot. (*C*–D) "GO" analysis of DEGs between two clusters. (E) "KEGG" analysis of DEGs between two clusters.

checkpoint blockade genes identified, including HAVCR2, PDCD1, LAG3, TIGIT, CD274, SIGLEC15, CTLA4 and PDCD1LG2 were significantly lower in cluster 1 ($p < 0.05$). Considering the significantly different OS curves of two clusters in BLCA mentioned above, we inferred tumor microenvironment might be a vigorous indicator to the tumor progression of BLCA. Through "ESTIMATE", we observed the immune score was strikingly lower in cluster 1 (Fig. 2C, $p < 0.05$). Also, the stromal and estimate score exhibited the same tendency (Fig. 2D–E, $p < 0.05$). Meanwhile, the tumor purity was compared, it indicated the purity was obviously higher in cluster 1 (Fig. 2F, $p < 0.05$). Overall, these findings powerfully revealed the clusters constructed with the ADFRMs were closely related to tumor microenvironment in BLCA.

3.3. Correlation analysis between ADFRMs with molecular characteristics

Total 3750 DEGs were identified between the two clusters in BLCA, including 991 up-regulated and 2759 down-regulated DEGs, and the 100 most significant DEGs were presented in Fig. 3A (**$|\log_2 FC|>1$, FDR<0.05**). And one volcano plot roughly showed these DEGs (Fig. 3B). To better understand the biological functions related to ADFRMs in BLCA, the "GO" enrichment analysis containing biological process, cellular component and molecular function was conducted based on the DEGs (Fig. 3C). We found that the DEGs based on the ADFRMs patterns were related to immunity and biological metabolism (Fig. 3D, $p < 0.05$). The "KEGG" pathway analysis was then carried out (Table 1), the results indicated various classical tumor-related signaling pathways were strikingly enriched, such as PI3K-Akt, MAPK and JAK-STAT signaling pathways (Fig. 3E, $p < 0.05$).

Meanwhile, the GSEA was carried out to investigate the 5 most concentrated signaling pathways of the DEGs. It demonstrated that DEGs in cluster 1 primarily enriched in the DRUG_METABOLISM_CYTOCHROME_P450, PENTOSE_AND_GLUCURONATE_INTER

CONVERSIONS and etc, DEGs in cluster 2 were related to CELL_ADHESION_MOLECULES_CAMS, CYTOKINE_CYTOKINE_RECEPTOR_INTERA

CTION and etc (Fig. 4A and B, $p < 0.05$). Further, we identified the differences of somatic genomic mutation between two clusters. The distribution of the top 20 most mutated genes were exhibited in Fig. 4C and D. Overall, the frequency of mutation in cluster 1 was much lower than cluster 2. Among of them, the rates of TTN, TP53, RYR2, EP300, RB1 and FAT4 mutation were obviously higher in cluster 2. However, 28 % of samples in cluster 1 had KDM6A mutations compared to 17 % in cluster 2 group. Moreover, we found missense was the most common type of mutation in both two clusters.

3.4. Construction of a prognostic model with ADFRMs

To investigate the potential prognostic capability of ADFRMs in BLCA, univariate Cox regression analysis was conducted. And 3 prognostic-related genes of ADFRMs were determined (Fig. 5A). The "Lasso" regression algorithm was then carried out to further identify key genes which have outstanding prognostic value (Fig. S1). Ultimately, TRIB3 and WIPI1 were determined and one prognostic model was established with the identified genes for BLCA. Then, the BLCA patients' risk score was formulated by calculating the expression level of TRIB3 and WIPI1 by their coefficients, and patients were separated into a low-risk or high-risk group by using a median risk score (Fig. 5E). The expression levels of TRIB3 and WIPI1 in low-risk and high-risk groups were displayed with a heatmap (Fig. 5B). In vitro, we verified the expression level of both TRIB3 and WIPI1 were up-regulated in BLCA cell line T24 compared with SV-HUC-1 via q-PCR (Fig. 5C and D). The scatter chart showed BLCA patients with a low risk score had a better prognosis (Fig. 5F). Besides, the survival analysis presented a similar result (Fig. 5G, $p = 0.003$). The efficiency of the model was assessed through "ROC" curve (Fig. 5H). Meanwhile, GSE13507 from GEO datebase was further applied to validate the model, it also indicated patients with a low risk score were prone to own a strikingly longer OS (Fig. 5I, $p = 0.018$). And one "ROC" curve was carried out to assess the model (Fig. 5J).

3.5. Correlation analysis between risk score with clinical characteristic

To validate whether the risk score developed could serve as an independent indicator for OS in BLCA, univariate and multivariate analysis were further conducted (Table 2). The univariate analysis indicated the age, clinical stage and the risk score were linked to a poor survival, and the multivariate analysis showed the same result (Fig. 6A and B, $p < 0.001$). Further, the correlation of risk score and the clinical characteristic including age, gender, grade, and stage was identified. The boxplot indicated that BLCA patient with stage III−IV, high grade, or age>65 was strongly correlated with a high risk score (Fig. 6C–E, $p < 0.05$). However, there was no significant difference between gender indicator and the risk score (Fig. 6F).

Table 1
Univariate and multivariate Cox analysis of riskScore and clinicopathologic characteristics in BLCA; Bold font means P value was less than 0.05

ID	Univariate cox regression analysis				Multivariate cox regression analysis			
	HR	HR.95L	HR.95H	p-value	HR	HR.95L	HR.95H	p-value
Age	1.034265	1.018164	1.050621	**0.000026**	1.029432	1.013208	1.045915	**0.000345**
Gender	0.886655	0.637065	1.234029	0.475702	0.847207	0.607103	1.182269	0.329459
Grade	2.870706	0.709982	11.607274	0.139021	0.990222	0.237913	4.121420	0.989225
Stage	1.741090	1.434094	2.113805	**0.000001**	1.639885	1.345432	1.998780	**0.000001**
riskScore	3.477289	1.925562	6.279486	**0.000036**	2.917158	1.585936	5.365799	**0.000575**

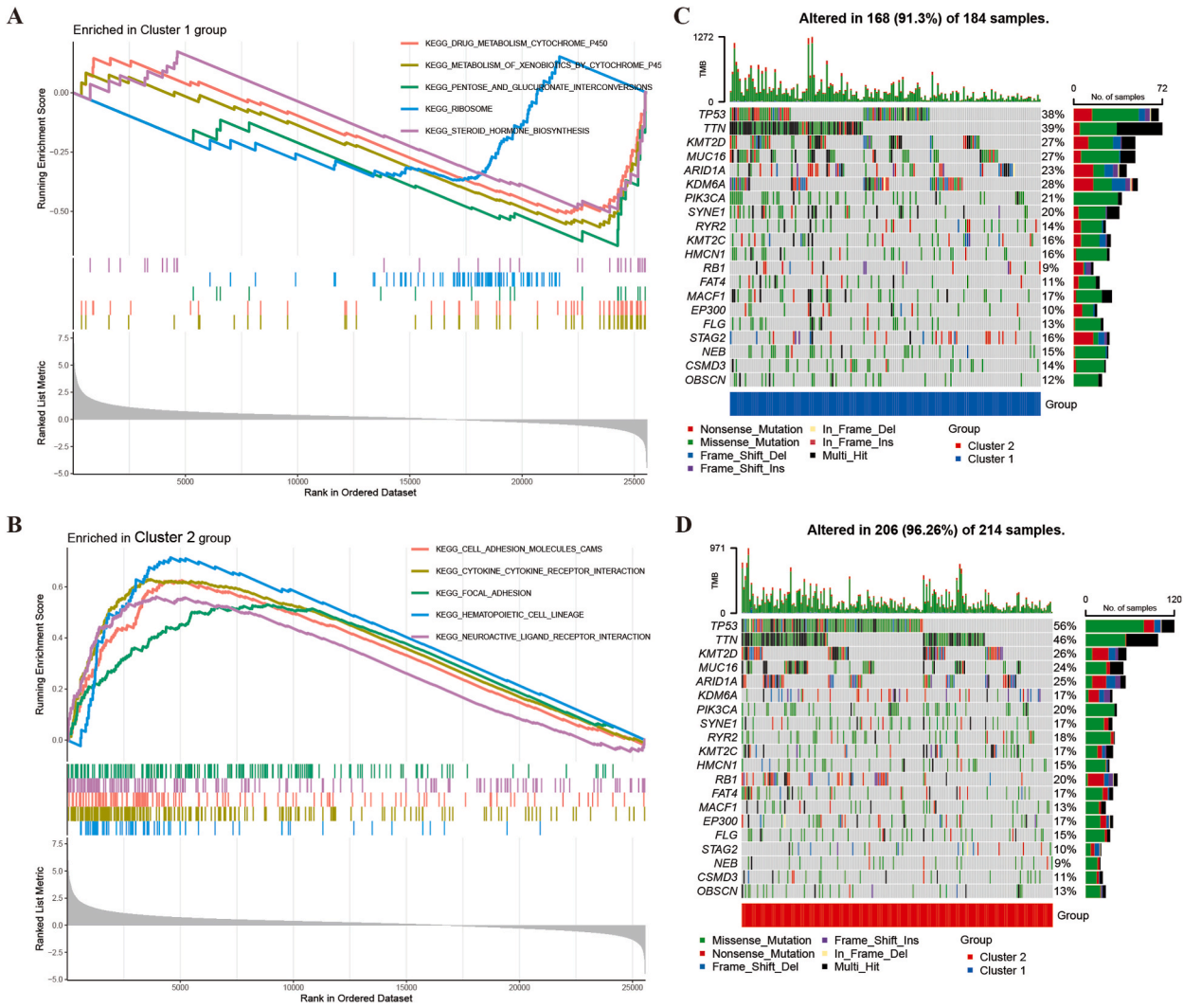

Fig. 4. Molecular characteristics analysis between two clusters. (A–B) "GSEA" of DEGs between two clusters. (*C*–D) The analysis of tumor somatic genomic mutation between two clusters.

3.6. Correlation analysis between risk score and tumor microenvironment

By using "ssGSEA", enrichment scores of different immune cell subsets in two groups were acquired. There was significant difference in the composition of aDCs, Macrophages, and Treg between two groups (Fig. 7A, $p < 0.05$). Furthermore, the scores of immune functions such as APC-co-inhibition, parainflammation and CCR were closely correlated to the risk score (Fig. 7B, $p < 0.05$). Six types of immune infiltration were applied for investigating the correlation with the risk score, including C1 (wound healing), C2 (IFN-g dominant), C3 (inflammatory), C4 (lymphocyte depleted), C5 (immunologically quiet), and C6 (transforming growth factor beta dominant), which were proved to play a vigorous role in the tumor repressing or promoting. There were no BLCA patient classified as C5 or C6, which were not covered in current study. Infiltration types of C1 and C2 tended to occur in patients in high-risk group, while C3 and C4 were prone to occur in low-risk group (Fig. 7C, $p < 0.05$).

Further, we investigated the immune cell infiltration view of patients in TCGA-BLCA dataset using the CIBERSORT algorithm. We found the risk score was positively related to the immune and stromal score in BLCA (Fig. 7D–E, $p < 0.05$). In addition, to investigate the response of established prognostic model to immunotherapy, the immune checkpoint blockade genes expression level of LAG3, PD-L1 and CTLA4 in different risk groups were assessed (Fig. 7F–K). Patients in high-risk group corresponded to a highly-expressed immune checkpoint molecular features compared to patients in low-risk group, which prone to benefit from the immune checkpoint inhibitor intervention.

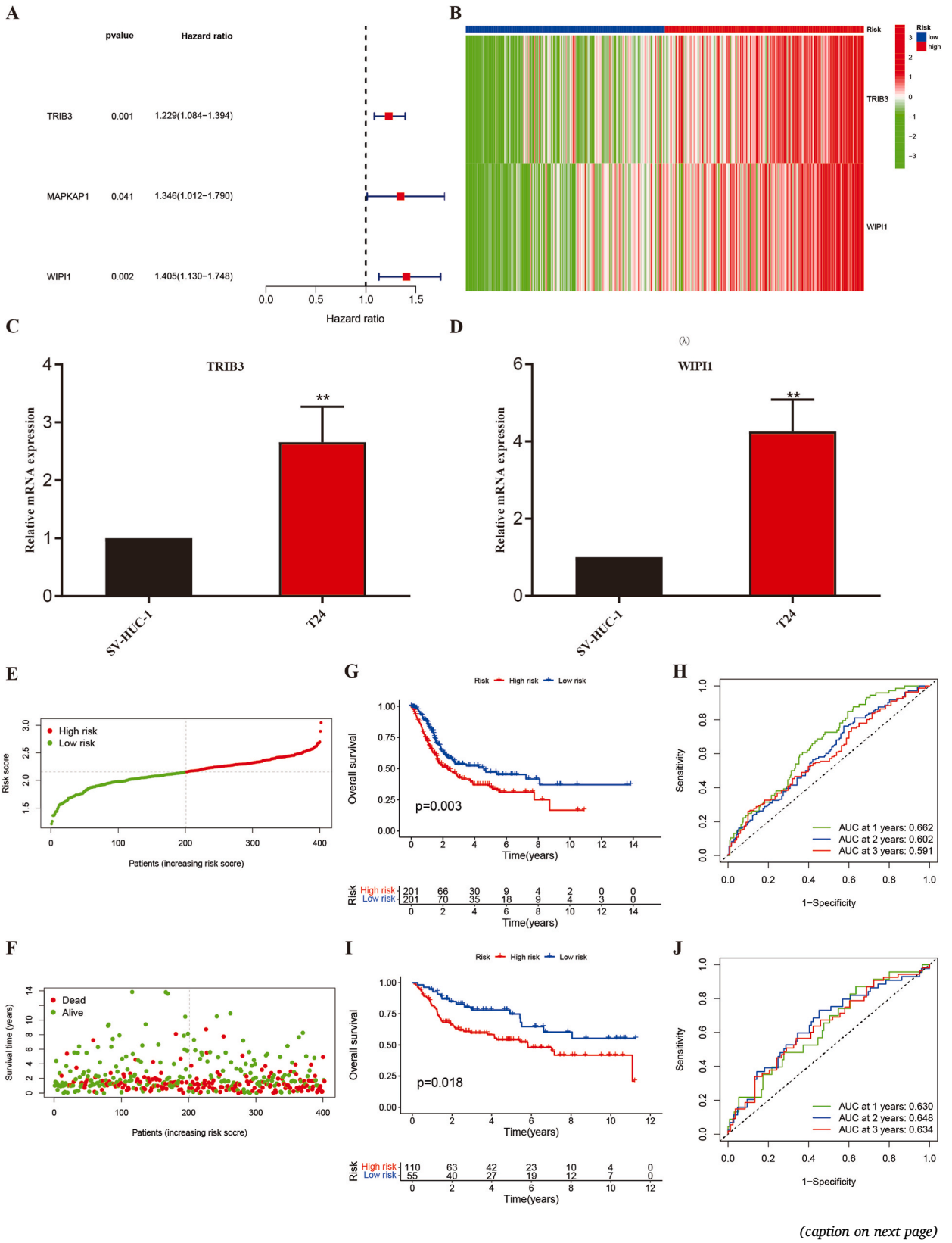

(caption on next page)

Fig. 5. Establishment of a prognostic model with ADFRM. (A) Forest plot of survival-associated genes by Univariate Cox regression analysis. (B) The expression level of two prognosis-related ADFRMs between two clusters with heatmap. (C–D) The expression of TRIB3 and WIPI1 of BLCA cell T24 compared with the normal bladder cell line SV-HUC-1. (*E*–F) The correlation of risk score distribution and the survival status of BLCA patients in TCGA. (G) "Kaplan-Meier" survival analysis in TCGA-BLCA court. (H) "ROC" curve for prediction of OS in TCGA-BLCA court. (I) "Kaplan-Meier" survival analysis in GSE13507 dataset. (K) "ROC" curve for prediction of OS in GSE13507 dataset.

Table 2
Gene set enrichment analysis results.

MSigDB collection	Gene set name	NES	NOM *P*-val	FDR q-val
c2.cp.kegg.v7.1 symbols.gmt	KEGG_DRUG_METABOLISM_CYTOCHROME_P450	−2.180	< 0.05	< 0.01
	KEGG_METABOLISM_OF_XENOBIOTICS_BY_CYTOCHROME_P450	−2.428	< 0.05	< 0.01
	KEGG_PENTOSE_AND_GLUCURONATE_INTERCONVERSIONS	−2.104	< 0.05	< 0.01
	KEGG_RIBOSOME	−1.725	< 0.05	< 0.01
	KEGG_STEROID_HORMONE_BIOSYNTHESIS	−1.906	< 0.05	< 0.01
	KEGG_CELL_ADHESION_MOLECULES_CAMS	2.203	< 0.05	< 0.01
	KEGG_CYTOKINE_CYTOKINE_RECEPTOR_INTERACTION	2.309	< 0.05	< 0.01
	KEGG_FOCAL_ADHESION	1.937	< 0.05	< 0.01
	KEGG_HEMATOPOIETIC_CELL_LINEAGE	2.329	< 0.05	< 0.01
	KEGG_NEUROACTIVE_LIGAND_RECEPTOR_INTERACTION	2.029	< 0.05	< 0.01

3.7. Correlation analysis between prognostic gene and sensitivity to chemotherapy

To learn the correlation of TRIB3 or WIPI1 and drug sensitivity, we identified their level in "NCI-60". As presented in Fig. 8A–I, the top 9 significant correlation analyses based on the p value were performed. We found the expression of TRIB3 in the samples was negatively associated with IC50 values of Acalabrutinib, and the expression of WIPI1 in the samples was positively associated with IC50 values of Vemurafenib, Dabrafenib, Ixazomib citrate, Bortezomib and etc. ($p < 0.01$). It indicated that patients with high TRIB3 expression was sensitive to Acalabrutinib inhibitor, while patients with low WIPI1 expression was sensitive to Vemurafenib, Dabrafenib, Ixazomib citrate, Bortezomib and etc.

4. Discussion

BLCA was one of the ten most common malignant neoplasms globally, which remained a thorny problem for clinicians as its high invasiveness and recurrence rate [16]. Nowadays, with the wide application of sequencing and analysis techniques, integrated analysis based on public databases have been developing in the identification of avenues for exploring promising diagnostic or prognostic biomarkers, therapeutic targets in BLCA[17–19]. Compared with traditional surgery and chemotherapy, it was of great value to implement the precise treatment for improving the prognosis of BLCA patients. Therefore, improving the understanding of molecular biology and genetics, identifying key molecules, and building predictive models with high stability and validity for BLCA were indispensable.

In recent years, autophagy and ferroptosis have been widely concerned, and great progress has been made in various tumor research. Autophagy was one mechanism through which cellular material was transported to lysosomes for degradation, which plays a dual role by inhibiting tumorigenesis while supporting tumor progression [20,21]. Ferroptosis was a newly discovered type of cell death with recognizing functions and unique properties participated in human health or diseases including the cancer [22]. The rapid advancing researches of autophagy or ferroptosis in cancer has boosted its application prospects in therapy of cancer. Interestingly, relevant evidences have shown that autophagy was involved in the ferroptosis process, which facilitated ferroptosis selective degradation of ferroptosis-related regulators, termed autophagy-dependent ferroptosis [9]. It suggested that the regulatory mechanism of autophagy-dependent ferroptosis may have a unique implication in the study of tumor progression and precision therapy. So far, many studies have reported the correlation between ferroptosis or autophagy related signatures with the BLCA, providing potential targets and theories for the ferroptosis or autophagy in tumorigenesis and targeted therapy in BLCA [23–25]. However, joint analysis of autophagy-related ferroptosis regulatory molecules (ADFRMs) for BLCA has not been reported so far, there was still little known on the relationship between ADFRMs signature with BLCA. Therefore, based on ADFRMs, this paper conducted various analysis in detailed to identify potential targets of ADFRMs in the diagnosis, prognosis and immunotherapy of BLCA.

In this article, in order to better identify the genes involving ADFRMs, the Venn diagrams was utilized to analyze 564 genes from the "FerrDb" dataset and 796 genes from the "HAMdb" dataset, and finally 119 ADFRMs genes were enrolled in current study. Further, the expression pattern of 119 ADFRMs between BLCA with normal samples was systematically studied. To better understand the relationship of ADFRMs in TCGA-BLCA, the consensus classification was utilized, and BLCA patients were grouped into two clusters by the expression level of ADFRMs.

The OS analysis indicated patients in cluster 1 had a good prognosis than that of patients in cluster 2. Increasing evidences suggested the prognosis of various tumors was intimately related to tumor microenvironment defined as the rich and complex multicellular environment, which typically comprised immune cells, stromal cells, the extracellular matrix (ECM) and so on [26–28]. In current study, patients in cluster 2 were found to have a higher estimate score, stromal score and immune score but a lower tumor

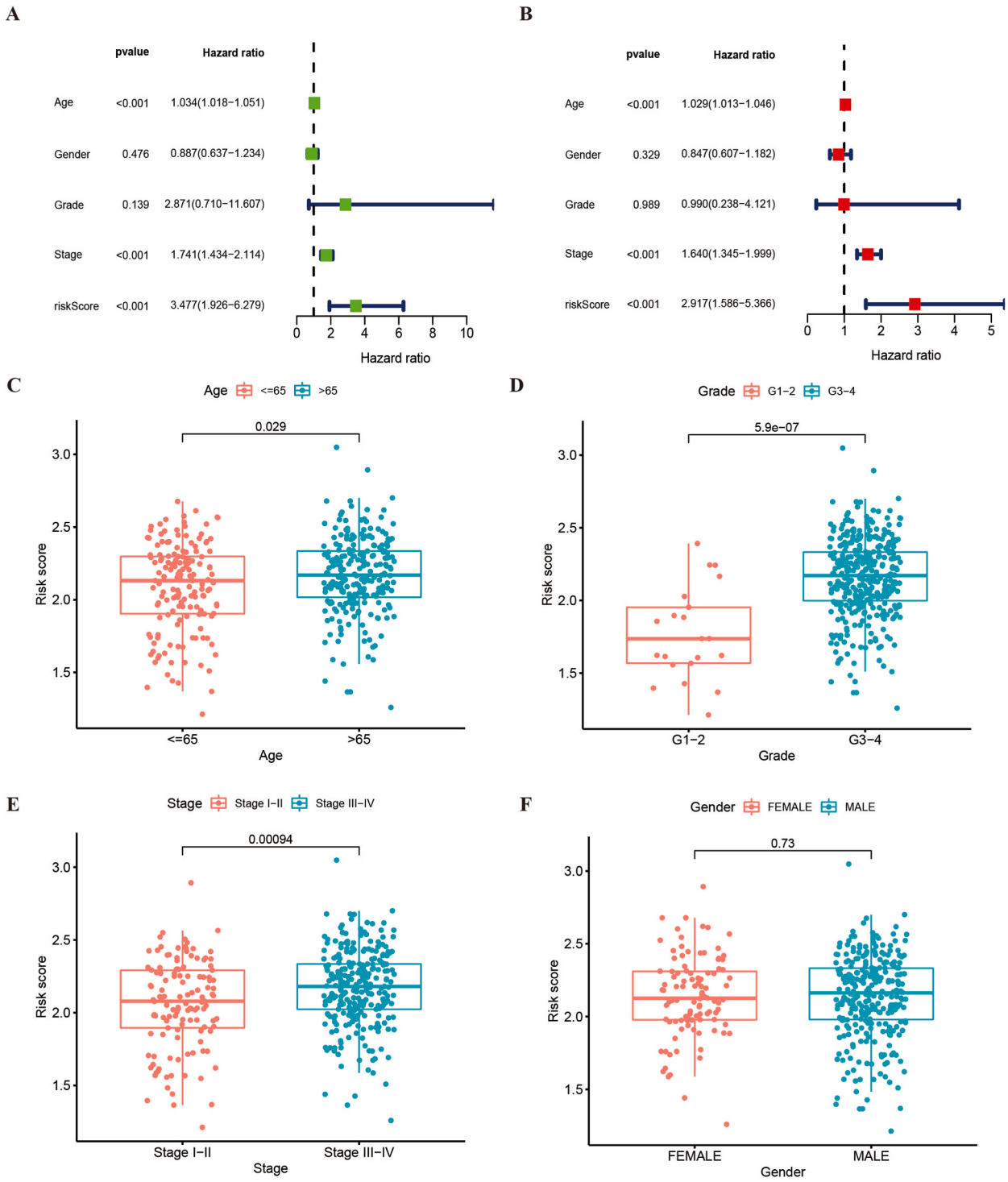

Fig. 6. Correlation analysis between risk score with clinical characteristic. (A–B) Univariate and multivariate cox regression analysis of risk score and clinicopathological characteristics. (*C*–F) The relationship of risk scores with age, grade, stage and gender.

purity. Previous studies revealed that high stromal, immune scores and estimate score, representing infiltrating of immune cells, which were correlated with a poor prognosis [29,30]. In addition, evidences have shown that tumor purity was negatively correlated with immune cell infiltration and the OS, and low tumor purity normally represents a poor prognosis [31,32], which was in consistent with our results. Furthermore, patients in cluster 2 also exhibited a lower expression level of naive B cells, plasma cells and T cells

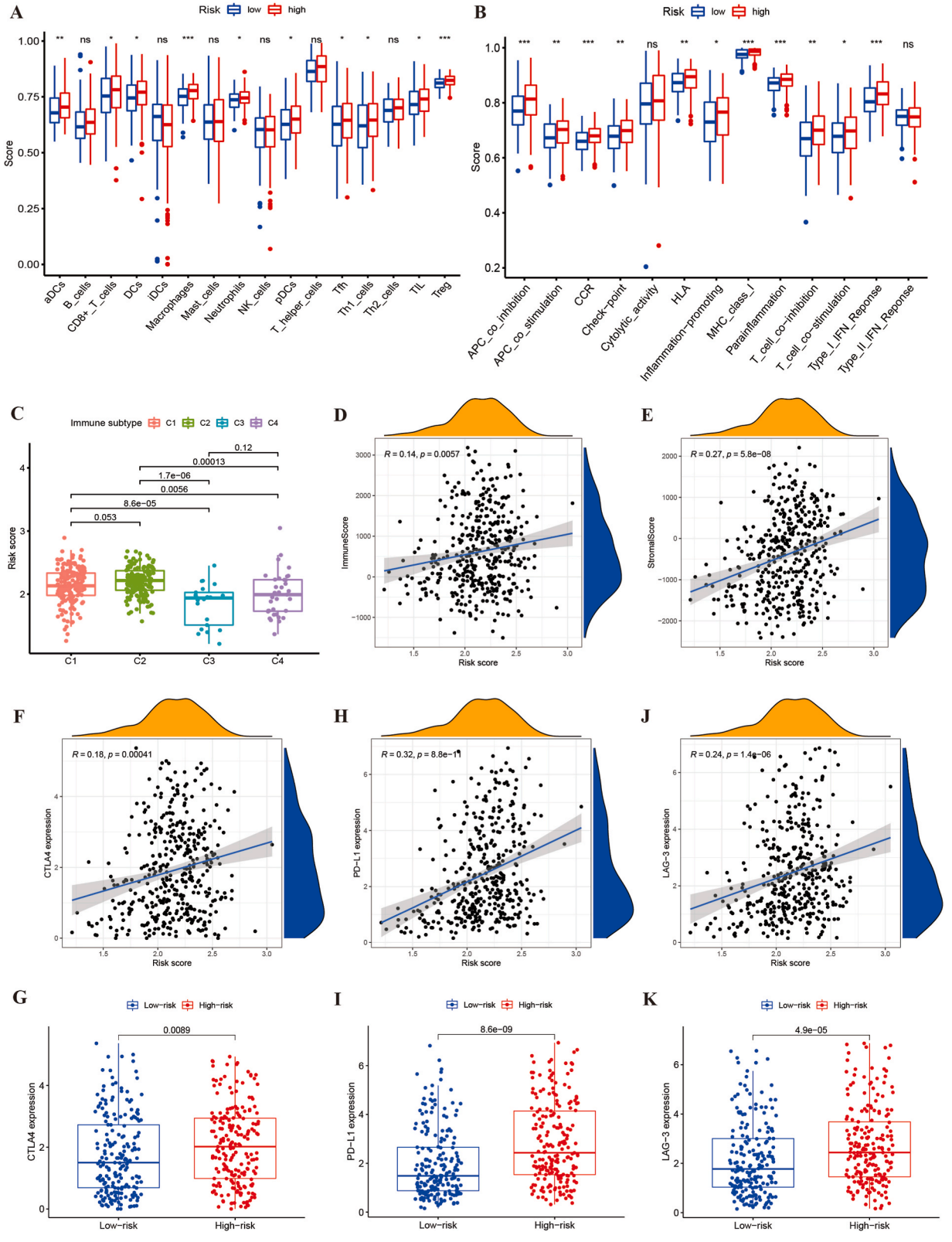

(caption on next page)

Fig. 7. Correlation analysis of tumor microenvironment with risk score in BLCA. (A–B) The boxplots showed the of immune genes and immune functions between different risk groups. (C) Correlation analysis of risk score with immune infiltration subtypes. (D–E) The correlation of risk score with immune score and stromal score. (H–K) Correlation analysis of risk score and immune checkpoint blockage genes including CTLA4, PDL-1 and LAG-3.

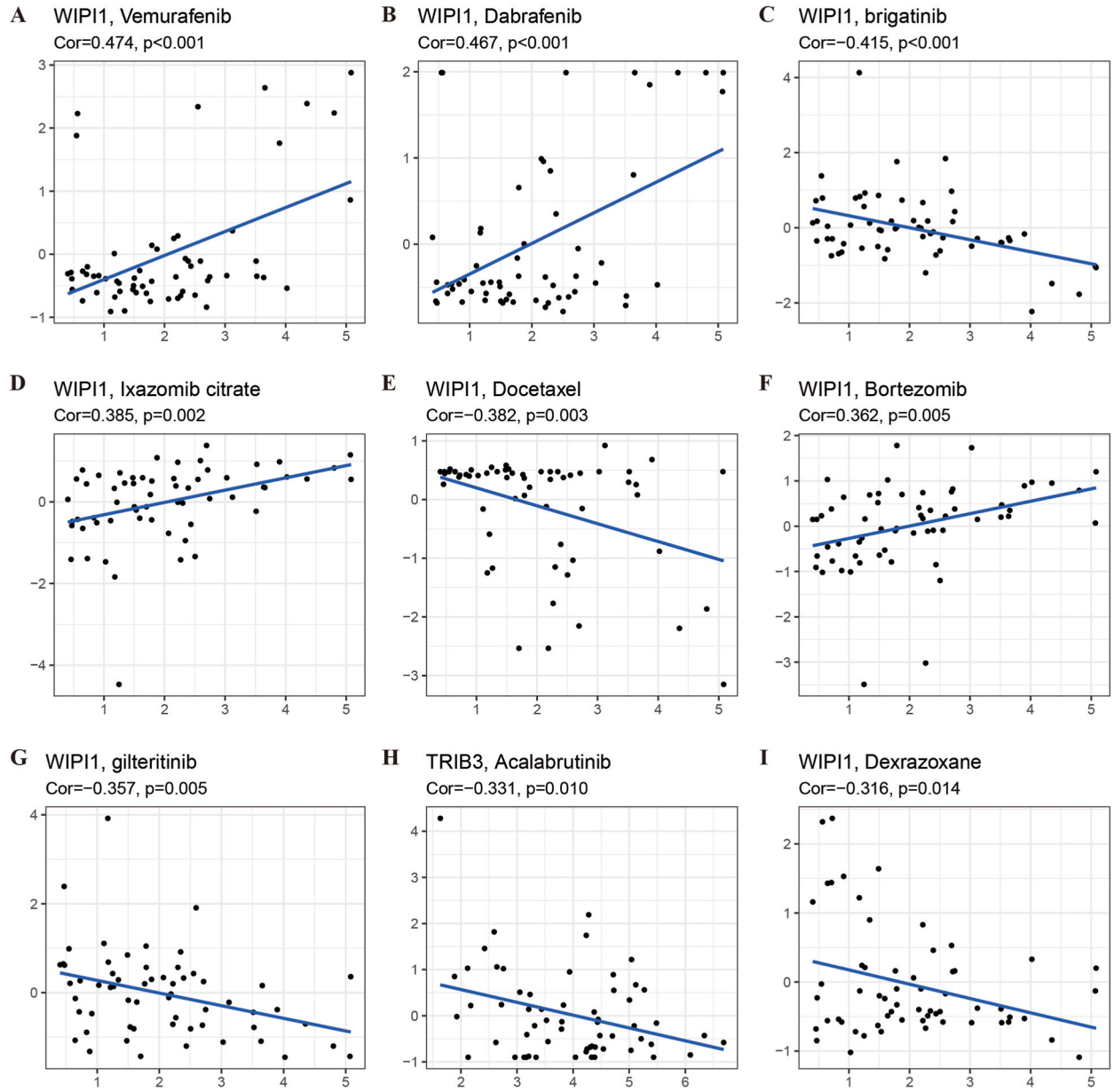

Fig. 8. Correlation analysis between drug sensitivity and prognostic gene expression. Association between prognostic gene expression and (A) Vemurafenib; (B) Dabrafenib; (C) brigatinib; (D) lxazomib citrate; (E) Docetaxel; (F) Botezomib; (G) gilteritinib; (H) Acalabrutinib; (I) Dexrazoxane.

regulatory, but a high expression levels of macrophages M1, which again witnessed the two groups divided by ADFRMs expression level were closely related to the tumor microenvironment. Several immune checkpoint blockage genes, such as CD274 and CTLA4, were highly-expressed in cluster 2 than in cluster 1. It suggested these patients in cluster 2 prone to benefit from the immune therapy, which potentially improve the BLCA patients with a poor prognosis by enhancing immune response or inducing the ferroptosis mediated by autophagy [33].

To further explore the potential function of ADFRMs in TCGA-BLCA court, 3750 DEGs were identified of two clusters, and we further analyzed its biological functions via “GO” annotation analysis. It indicated the DEGs mainly enriched in biological process such

as epidermis development and leukocyte migration, celler component such as presynapse and neuronal cell body, molecular function such as receptor ligand and cytokine activity. To further investigate potential pathways of how the ADFRMs mediated the progression of BLCA, "KEGG" and "GSEA" were performed respectively. It indicated the DEGs enriched in the following signaling pathways, for instance, JAK-STAT, MAPK, PI3K/AKT and so on. The PI3K/AKT and JAK-STAT pathways have been proved to play a vital role in regulation of occurrence, migration and infiltration for BLCA [34,35] and the MAPK pathway was tightly correlated with the occurrence and progression of various tumors which had a great potential role in tumor therapy [36,37]. GSEA suggested DEGs in cluster 1 were enriched in drug metabolism cytochrome P450, ribosome and etc, and DEGs in cluster 2 were enriched in cytokine receptor interaction, cell adhesion molecules and so on. Briefly, we suspected that the autophagy-dependent ferroptosis might be suppressed in cluster 2 through pathways mentioned above. These findings provided direction for understanding the role of autophagy-dependent ferroptosis and the possible regulatory molecular mechanisms in BLCA.

Furthermore, a reliable prognostic model based on ADFRMs including TRIB3 and WIPI1 was established by Lasso regression analysis. The BLCA patients were divided into a low-risk and a high-risk group with the median risk score. The OS analysis and ROC curve were performed to investigate the predictive capability of this prognostic model, and we further verified it using one external dataset. Notably, the model was probably easier to applied into the clinic than others attributed to only 2 ADFRMs were included. Correlation analysis between risk score and clinical characteristic indicated the risk score was positively correlated to age, tumor garde and stage. Moreover, univariate and multivariate analysis of regression both indicated it could be an independent prognostic signature, and BLCA patients with a high risk score tended to have a poor prognosis.

Ferroptosis was proved to have great potential in suppressing the occurrence and progression of tumors. However, the ferroptosis could also provide a favorable environment for promoting tumor progression, due to the infiltration of immune cells related to tumor promoting, or the dysfunction of immune function related to anti-tumor [38,39]. We have conducted the correlation analysis of ADFRMs with the tumor microenvironment in BLCA, and we also carried out the correlation analysis of immune cell infiltration on the established prognostic model based on ADFRMs. As expected, the risk score showed a strong correlation with tumor microenvironment including immune cells, immune subtypes, immune score and immune checkpoint blockage genes. It once again proved that ADFRMs were strongly correlated to the tumor microenvironment of BLCA, which may play an indispensable role in tumor occurrence, progression or tumor suppression. Meanwhile, ADFRMs had potential immunotherapy effects in BLCA, especially for those patients with poor prognosis. Further, two genes TRIB3 and WIPI1 were identified and included in the model. We noticed both the TRIB3 and WIPI1 were up-regulated in BLCA. In vitro, we verified that both TRIB3 and WIPI were up-regulated in BLCA cell line T24 relative to normal bladder cell line SV-HUC-1. *Yang* et al. indicated high expression level of TRIB3 was correlated with advanced stage or grade and the poor OS [40]. *Shang* et al. claimed TRIB3 could induce immune evasion by reducing immune cell infiltration in colorectal cancer, and it could facilitate glioblastoma progression via restraining autophagy [41,42]. Similarly, WIPI1 was confirmed to promote osteosarcoma cell proliferation through inhibiting CDKN1A, and the detection of WIPI1 could be a convenient method of monitoring autophagosome formation in different cells [43,44]. We speculated that abnormally high expression of WIPI1 or TRIB3, as one key gene related to autophagy, may affect the occurrence and progression of autophagy-dependent ferroptosis. Further experiments are required to prove the speculation.

In addition, we explored the correlation of TRIB3 or WIPI1 expression level with drug sensitivity in BLCA by the "CellMiner" platform. Our findings suggested that WIPI1 expression showed positive correlation with the IC50 of Vemurafenib, Dabrafenib, Ixazomib citrate, Bortezomib, and etc. It means that in BLCA, patients with low expression of WIPI1 were prone to benefit from these molecular drugs therapy. Meanwhile, WIPI1 expression showed negative correlation with the inhibitors of Brigatinib, Docetaxel and gilteritinib, while TRIB3 expression showed negative correlation with the IC50 of Acalabrutinib. It means that in BLCA, patients with high expression of WIPI1 or TRIB3 were prone to benefit from these molecular drugs therapy. These discoveries provided a basis to explore the targeting effect of TRIB3 and WIPI1 on tumor immunity and molecular therapy.

However, the current study still has several limitations, we have not further investigated the function and molecular mechanism of ADFRMs for BLCA. Besides, the value of autophagy-dependent ferroptosis mechanism in immunotherapy intervention for BLCA still needs further clinical trials to verify.

5. Conclusions

It was the first time to investigate the relationship of ADFRMs with BLCA. The current study revealed BLCA patients could be grouped into two clusters via the ADFRMs expression pattern, and the two clusters were closely related to the OS, tumor microenvironment and biological functions. Further, a reliable prognostic predictive model was construct with TRIB3 and WIPI1, which was relatively easy to apply into clinical BLCA patients. These findings provided several valuable insights into predicting the prognosis for BLCA patients based on the autophagy-dependent ferroptosis pathway, and may even be helpful for the clinical immunotherapeutic intervention of BLCA.

Funding

None declared.

Author contributions

Shiwei Liu: Analyzed and interpreted the data; Wrote the paper.

Jing Zhai: Contributed reagents and materials; Wrote the paper.
Deng Li: Contributed reagents and materials.
Yu Peng: Performed the experiments.
Yi Wang: Performed the experiments; Analyzed and interpreted the data.
Bo Dai: Conceived and designed the experiments.

Data availability statement

The total RNA-seq and the clinical data of TCGA-BLCA dataset and GSE13507 dataset acquired from TCGA database (http://cancergenome.nih.gov/) and GEO (https://www.ncbi.nlm.nih.gov/geo/) respectively. The "ADFRMs" set was identified from two online databases, including the "HAMdb" (hamdb.scbdd.com/home/index/) and the "FerrDb" (www.zhounan.org/ferrdb/current/).

Ethics approval and consent to participate

The current research was approved by the Institutional Review Board of Shanghai General Hospital and all patients signed an informed consent form.

Consent for publication

Not applicable.

Declaration of competing interest

The authors declare that they have no known competing financial interests or personal relationships that could have appeared to influence the work reported in this paper.

Acknowledgements

None declared.

Appendix A. Supplementary data

Supplementary data to this article can be found online at https://doi.org/10.1016/j.heliyon.2023.e21092.

References

[1] R.L. Siegel, K.D. Miller, H.E. Fuchs, A. Jemal, Cancer statistics, 2022, CA Cancer J Clin 72 (2022) 7–33.
[2] C. Xia, X. Dong, H. Li, M. Cao, D. Sun, S. He, et al., Cancer statistics in China and United States, 2022: profiles, trends, and determinants, Chin Med J (Engl) 135 (2022) 584–590.
[3] A.M. Kamat, N.M. Hahn, J.A. Efstathiou, S.P. Lerner, P.U. Malmstrom, W. Choi, et al., Bladder cancer, Lancet (N. Am. Ed.) 388 (2016) 2796–2810.
[4] V.G. Patel, W.K. Oh, M.D. Galsky, Treatment of muscle-invasive and advanced bladder cancer in 2020, CA Cancer J Clin 70 (2020) 404–423.
[5] A.T. Lenis, P.M. Lec, K. Chamie, M.D. Mshs, Bladder cancer: a Review, JAMA 324 (2020) 1980–1991.
[6] S.J. Dixon, K.M. Lemberg, M.R. Lamprecht, R. Skouta, E.M. Zaitsev, C.E. Gleason, et al., Ferroptosis: an iron-dependent form of nonapoptotic cell death, CELL 149 (2012) 1060–1072.
[7] H.F. Yan, T. Zou, Q.Z. Tuo, S. Xu, H. Li, A.A. Belaidi, et al., Ferroptosis: mechanisms and links with diseases, Signal Transduct. Targeted Ther. 6 (2021) 49.
[8] G. Lei, L. Zhuang, B. Gan, Targeting ferroptosis as a vulnerability in cancer, Nat. Rev. Cancer 22 (2022) 381–396.
[9] B. Zhou, J. Liu, R. Kang, D.J. Klionsky, G. Kroemer, D. Tang, Ferroptosis is a type of autophagy-dependent cell death, Semin. Cancer Biol. 66 (2020) 89–100.
[10] R. Kang, D. Tang, Autophagy and ferroptosis - what's the connection? Curr Pathobiol Rep 5 (2017) 153–159.
[11] J. Liu, F. Kuang, G. Kroemer, D.J. Klionsky, R. Kang, D. Tang, Autophagy-dependent ferroptosis: machinery and regulation, Cell Chem. Biol. 27 (2020) 420–435.
[12] R. Shi, X. Bao, K. Unger, J. Sun, S. Lu, F. Manapov, et al., Identification and validation of hypoxia-derived gene signatures to predict clinical outcomes and therapeutic responses in stage I lung adenocarcinoma patients, THERANOSTICS 11 (2021) 5061–5076.
[13] M.D. Wilkerson, D.N. Hayes, ConsensusClusterPlus: a class discovery tool with confidence assessments and item tracking, BIOINFORMATICS 26 (2010) 1572–1573.
[14] A. Subramanian, P. Tamayo, V.K. Mootha, S. Mukherjee, B.L. Ebert, M.A. Gillette, et al., Gene set enrichment analysis: a knowledge-based approach for interpreting genome-wide expression profiles, Proc Natl Acad Sci U S A 102 (2005) 15545–15550.
[15] T. Li, J. Fan, B. Wang, N. Traugh, Q. Chen, J.S. Liu, et al., TIMER: a web server for comprehensive analysis of tumor-infiltrating immune cells, Cancer Res. 77 (2017) e108–e110.
[16] L. Tran, J.F. Xiao, N. Agarwal, J.E. Duex, D. Theodorescu, Advances in bladder cancer biology and therapy, Nat. Rev. Cancer 21 (2021) 104–121.
[17] Z. Xu, H. Chen, J. Sun, W. Mao, S. Chen, M. Chen, Multi-Omics analysis identifies a lncRNA-related prognostic signature to predict bladder cancer recurrence, Bioengineered 12 (2021) 11108–11125.
[18] L.H. Zhang, L.Q. Li, Y.H. Zhan, Z.W. Zhu, X.P. Zhang, Identification of an IRGP signature to predict prognosis and immunotherapeutic efficiency in bladder cancer, Front. Mol. Biosci. 8 (2021), 607090.
[19] Z. Lv, C. Pang, J. Wang, H. Xia, J. Liu, Q. Yan, et al., Identification of a prognostic signature based on immune-related genes in bladder cancer, Genomics 113 (2021) 1203–1218.
[20] A.V. Onorati, M. Dyczynski, R. Ojha, R.K. Amaravadi, Targeting autophagy in cancer, CANCER-AM CANCER SOC 124 (2018) 3307–3318.

[21] J. Levy, C.G. Towers, A. Thorburn, Targeting autophagy in cancer, Nat. Rev. Cancer 17 (2017) 528–542.
[22] Y. Mou, J. Wang, J. Wu, D. He, C. Zhang, C. Duan, et al., Ferroptosis, a new form of cell death: opportunities and challenges in cancer, J. Hematol. Oncol. 12 (2019) 34.
[23] R. Cao, B. Ma, G. Wang, Y. Xiong, Y. Tian, L. Yuan, Identification of autophagy-related genes signature predicts chemotherapeutic and immunotherapeutic efficiency in bladder cancer (BLCA), J. Cell Mol. Med. 25 (2021) 5417–5433.
[24] L. Yang, C. Li, Y. Qin, G. Zhang, B. Zhao, Z. Wang, et al., A novel prognostic model based on ferroptosis-related gene signature for bladder cancer, Front. Oncol. 11 (2021), 686044.
[25] J. Sun, W. Yue, J. You, X. Wei, Y. Huang, Z. Ling, et al., Identification of a novel ferroptosis-related gene prognostic signature in bladder cancer, Front. Oncol. 11 (2021), 730716.
[26] L. Bejarano, M. Jordao, J.A. Joyce, Therapeutic targeting of the tumor microenvironment, Cancer Discov. 11 (2021) 933–959.
[27] J.E. Bader, K. Voss, J.C. Rathmell, Targeting metabolism to improve the tumor microenvironment for cancer immunotherapy, Mol. Cell. 78 (2020) 1019–1033.
[28] C. Roma-Rodrigues, R. Mendes, P.V. Baptista, A.R. Fernandes, Targeting tumor microenvironment for cancer therapy, Int. J. Mol. Sci. 20 (2019).
[29] Z. Wu, Z. Lu, L. Li, M. Ma, F. Long, R. Wu, et al., Identification and validation of ferroptosis-related LncRNA signatures as a novel prognostic model for colon cancer, Front. Immunol. 12 (2021), 783362.
[30] C. Zhang, J.H. Zheng, Z.H. Lin, H.Y. Lv, Z.M. Ye, Y.P. Chen, et al., Profiles of immune cell infiltration and immune-related genes in the tumor microenvironment of osteosarcoma, Aging (Albany NY) 12 (2020) 3486–3501.
[31] Y. Deng, Z. Song, L. Huang, Z. Guo, B. Tong, M. Sun, et al., Tumor purity as a prognosis and immunotherapy relevant feature in cervical cancer, Aging (Albany NY) 13 (2021) 24768–24785.
[32] Z. Gong, J. Zhang, W. Guo, Tumor purity as a prognosis and immunotherapy relevant feature in gastric cancer, Cancer Med. 9 (2020) 9052–9063.
[33] R. Cristescu, R. Mogg, M. Ayers, A. Albright, E. Murphy, J. Yearley, et al., Pan-tumor genomic biomarkers for PD-1 checkpoint blockade-based immunotherapy, Science (2018) 362.
[34] S. Yu, S. Wang, X. Sun, Y. Wu, J. Zhao, J. Liu, et al., ST8SIA1 inhibits the proliferation, migration and invasion of bladder cancer cells by blocking the JAK/STAT signaling pathway, Oncol. Lett. 22 (2021) 736.
[35] A. Sathe, R. Nawroth, Targeting the PI3K/AKT/mTOR pathway in bladder cancer, Methods Mol. Biol. 1655 (2018) 335–350.
[36] J. Wei, R. Liu, X. Hu, T. Liang, Z. Zhou, Z. Huang, MAPK signaling pathway-targeted marine compounds in cancer therapy, J. Cancer Res. Clin. Oncol. 147 (2021) 3–22.
[37] S. Lee, J. Rauch, W. Kolch, Targeting MAPK signaling in cancer: mechanisms of drug resistance and sensitivity, Int. J. Mol. Sci. 21 (2020).
[38] Q. Bi, Z.J. Sun, J.Y. Wu, W. Wang, Ferroptosis-mediated formation of tumor-promoting immune microenvironment, Front. Oncol. 12 (2022), 868639.
[39] K. Hadian, B.R. Stockwell, SnapShot: ferroptosis, CELL 181 (2020) 1188.
[40] J. Yang, J. Lin, J. An, Y. Zhao, S. Jing, M. Yu, et al., TRIB3 promotes the malignant progression of bladder cancer: an integrated analysis of bioinformatics and in vitro experiments, Front. Genet. 12 (2021), 649208.
[41] S. Shang, Y.W. Yang, F. Chen, L. Yu, S.H. Shen, K. Li, et al., TRIB3 reduces CD8(+) T cell infiltration and induces immune evasion by repressing the STAT1-CXCL10 axis in colorectal cancer, Sci. Transl. Med. 14 (2022) f992.
[42] Z. Tang, H. Chen, D. Zhong, W. Wei, L. Liu, Q. Duan, et al., TRIB3 facilitates glioblastoma progression via restraining autophagy, Aging (Albany NY) 12 (2020) 25020–25034.
[43] T. Ran, S. Ke, X. Song, T. Ma, Y. Xu, M. Wang, WIPI1 promotes osteosarcoma cell proliferation by inhibiting CDKN1A, Gene 782 (2021), 145537.
[44] S. Tsuyuki, M. Takabayashi, M. Kawazu, K. Kudo, A. Watanabe, Y. Nagata, et al., Detection of WIPI1 mRNA as an indicator of autophagosome formation, Autophagy 10 (2014) 497–513.